Journal of Agricultural Engineering

https://www.agroengineering.org/

Design and experiment of air-suction precision seed discharging device for wheat

Hong Hu,[1] Jun Chen,[2] Guanyue Zhang,[2] Ziqiang Wu[2]

[1]Modern Agricultural Equipment Research Institute;
[2]School of Mechanical Engineering, Xihua University, Chengdu, Sichuan, China

Corresponding author: Jun Chen, School of Mechanical Engineering, Xihua University, No. 999 Jinzhou Rd., Jinniu District, 610039 Chengdu, Sichuan, China. E-mail: 212022080200003@stu.xhu.edu.cn

Please cite this article as doi: 10.4081/jae.2025.1828

Submitted: 23 October 2024
Accepted: 6 May 2025

Design and experiment of air-suction precision seed discharging device for wheat

Hong Hu,[1] Jun Chen,[2] Guanyue Zhang,[2] Ziqiang Wu[2]

[1]Modern Agricultural Equipment Research Institute;
[2]School of Mechanical Engineering, Xihua University, Chengdu, Sichuan, China

Corresponding Author: Jun Chen, School of Mechanical Engineering, Xihua University, No. 999 Jinzhou Rd., Jinniu District, 610039 Chengdu, Sichuan, China. E-mail: 212022080200003@stu.xhu.edu.cn

Contributions: all authors made a substantive intellectual contribution, read and approved the final version of the manuscript and agreed to be accountable for all aspects of the work.

Conflict of interest: the authors declare no competing interests, and all authors confirm accuracy.

Abstract

A pneumatic precision wheat seed metering device was designed to improve the uniformity of wheat sowing. The structure and working principle of the seed metering device were described, and the effects of the shape, diameter, depth, number, and distribution of seed-distributing holes on the negative pressure at the seed-distributing holes were analyzed, leading to the determination of the optimal working parameters. The factors directly influencing the negative pressure at the seed-distributing holes were identified through an analysis of the forces acting on the seeds in the seed filling zone. A prototype of the seed metering device was fabricated and subjected to bench tests. The designed seed metering device achieved a qualified rate of 90.7%, a replanting rate of 4.8%, and a missed sowing rate of 4.5%, meeting the agronomic requirements for wheat sowing. This study provides theoretical guidance and parametric references for the design of future pneumatic wheat seed metering devices.

Key words: air-suction; precision; seed dispenser; wheat.

Introduction

Wheat, as one of the most crucial staple crops globally (Yu, 2009; Zhang *et al*., 2018), serves as the primary food source for nearly one-third of the world's population. Precision sowing, an agricultural technology that significantly enhances planting efficiency and crop yields, has become a key research area for professionals within the agricultural machinery industry worldwide. As a core component of precision sowing technology, seed metering devices are

classified into mechanical and pneumatic types based on their operational principles (Li *et al*., 2023). Compared to mechanical seed metering devices, pneumatic seed metering devices are characterized by their ability to prevent seed damage and their suitability for high-speed, precision sowing operations, making them increasingly popular (Li *et al*., 2025; Tang *et al*., 2023). However, research into optimizing the use of such devices remains limited.

Guarella and colleagues (1996) conducted both theoretical and experimental investigations into the pneumatic seed metering device for small-sized seeds, determining the optimal air pressure values for seed-distributing disks with varying hole diameters. To address the poor sowing performance of pneumatic seed metering devices, Singh *et al.* (2005) optimized the structural design and validated, through field trials, that the improved seed metering device met the sowing requirements for large-scale field operations. Li and his team (2015) developed a pneumatic seed metering device for oilseed crops, utilizing a self-designed "inverted square cone" hole configuration in the seed-distributing drum, coupled with a combined airflow seed cleaning and air pressure seed protection mechanism. Wang *et al*. (2009) designed a dual-suction-hole pneumatic drum-type seed metering device and conducted experiments to optimize and adjust the device's operational parameters. Shi and his team (2020) developed a precise seeding device featuring an automatic reseeding mechanism, which can autonomously reseed, thus significantly improving the seeding quality. Xing *et al*. (2015) introduced a layered seed filling chamber to enhance the seed flowability within the seed box, thereby improving the seed disc's ability to adsorb seeds. While these studies provide insights into the optimization of air pressure and seed metering device structures, there is limited research addressing the combined effects of these factors. The interactions between air pressure, the shape, diameter, depth, and number of seed-distributing holes, and their collective influence on the performance of the seed metering device remain underexplored. Additionally, there is a lack of detailed discussion on how the working parameters affect the operational efficiency of the seed metering device.

This study aims to design a pneumatic precision wheat seed metering device. The structural parameters of the seed-distributing disk, including hole shape, depth, diameter, number, and airflow slot width, have been optimized. The paper systematically investigates the impact of three key operational parameters -disc rotation speed, negative pressure, and the tilting angle of the disk- on seed dispensing performance, ultimately determining the optimal working parameters for the device.

Materials and Methods

Experimental materials

The experimental seeds used were *Chuanmai 104* wheat seeds, which are commonly used in the Sichuan region of China and are representative of local wheat varieties. The pneumatic

precision wheat seed metering device mainly consists of a seed box, seed-distributing disk, negative pressure chamber, and seed metering shaft, with its structure shown in Figure 1.

Experimental method

By measuring the physical parameters of the wheat seeds, the basic physical properties of the wheat were obtained. These data serve as the parametric basis for subsequent simulation experiments.

Determination of basic physical parameters of wheat seeds

Through the measurement of multiple groups of wheat seeds, the basic physical parameters of the wheat seeds were obtained (Jadhav *et al*., 2020; Yasir *et al*., 2012). The average three-axis dimensions (length × width × height) of the wheat seeds, measured using a digital caliper, were found to be 6.48 × 3.58 × 3.13 mm. The thousand-grain weight of the wheat seeds, measured using an electronic balance, was 49.21 g. The density of the wheat seeds was determined to be 0.243 g/cm³ using the drainage method. The moisture content of the wheat seeds was measured to be 7.58% using the drying method, as per GB/T 3453.6 standards. The shear modulus and Poisson's ratio of the wheat seeds were obtained as 18.31 MPa and 0.26, respectively, using a CMT1103 universal testing machine and the following formula.

$$\begin{cases} E = \dfrac{F/A}{\delta/L} \\ G = \dfrac{F_j/S}{T_0/T} \\ \mu = \dfrac{E}{2G} - 1 \end{cases} \quad \text{(Eq. 1)}$$

where: E is the elastic modulus; F is the normal force; A is the contact cross-sectional area between the wheat seed and the test machine's compressing surface; δ is the axial deformation of the seed under force; L is the initial axial length of the seed when no force is applied; F_j is the shear force; T_o is the depth at which the seed is penetrated by the tool; T is the thickness of the seed; and μ is the Poisson's ratio of the seed. Since the seed metering device is made from aluminum alloy and 45 steel, the static and kinetic friction coefficients of the wheat seeds were measured by placing the seeds on inclined surfaces made from these materials. In the static friction coefficient measurement, the wheat seed was placed stationary on the material plate, and the plate was gradually raised until the seed began to move. The angle between the plate and the horizontal surface at this point was recorded.

$\mu_2 = \tan \alpha$ (Eq. 2)

In the equation, μ_2 represents the static friction coefficient, and α is the angle of the inclined surface when the seed tends to slide.

The method for measuring the kinetic friction coefficient is similar to that for the static friction coefficient, except that in this case, the seed is initially placed on an inclined surface with a certain angle. Due to gravity, the seed rolls down the inclined surface. This process is recorded using a high-speed camera. The initial position of the seed is marked as point 1, a certain point during the seed's motion is marked as point 2, and the next frame, showing the position of the seed after it has moved further along the surface, is marked as point 3. The kinetic friction coefficient of the seed with different materials is calculated using the following formula:

$$\begin{cases} mgh_1 - mgh_2 - \dfrac{1}{2}mv^2 = \mu_1 mgs\cos\theta \\ v = \dfrac{\Delta s}{\Delta t} \end{cases} \quad \text{(Eq. 3)}$$

In the equation, m represents the mass of the seed, g is the gravitational acceleration, h_1 is the vertical height of the seed's initial position, h_2 is the vertical height at point 2, v is the speed of the seed at point 2, s is the distance between point 1 and point 2, μ_1 is the kinetic friction coefficient, Δs is the displacement between point 2 and point 3, and Δt is the time interval between point 2 and point 3.

The seed's restitution coefficient with different materials is determined by the ratio of the height the seed rebounds after falling from a certain height to the height from which it was dropped. This process is recorded using a high-speed camera. The restitution coefficient is then calculated using the following formula:

$$e = \frac{v_e}{v_s} = \sqrt{\frac{2gH_e}{2gH_s}} = \sqrt{\frac{H_e}{H_s}} \quad \text{(Eq. 4)}$$

In the equation, e is the coefficient of restitution, v_e is the velocity of the seed after colliding with the material, v_s is the velocity of the seed before collision, g is the gravitational acceleration, H_e is the maximum height the seed rebounds to after collision, and H_s is the initial drop height of the seed.

The measured coefficient of restitution, kinetic friction coefficient, and static friction coefficient for seed-seed, seed-aluminum alloy, and seed-45 steel are 0.308, 0.0978, 0.682, 0.332, 0.0761, 0.422, 0.439, 0.0634, and 0.449, respectively.

Seed particle model

By observing the shape of the wheat seeds and measuring their three-axis dimensions, a 3D model of the wheat seed was created. The model was then imported into EDEM software, where the software's default spherical particle filling method was used to establish the seed particle model (Figure 2).

Seed metering disc design

In traditional pneumatic seed metering devices, two types of seed-distributing holes are typically selected based on the characteristics of the seeds: when the seeds are lightweight, have minimal shape variation, and do not require high vacuum levels, a flat-shaped hole can be used; whereas, when the seeds are heavier, exhibit greater shape variation, and require mechanical assistance for seed suction, mechanical structures such as scoop-shaped holes or frustum-shaped holes are more appropriate (Chen *et al*., 2019; Leng *et al*., 2023; Zhu *et al*., 2023).

Due to the small size, light weight, and relatively regular shape of wheat seeds, the holes on the seed metering disc can be designed as flat suction holes. The schematic diagram of the seed metering disc structure is shown in Figure 3. In the diagram, the diameter of the installation hole is denoted as d_1, the distance between the holes and the center of the seed metering disc is d_2, the diameter of the holes is d_3, the diameter of the seed metering disc is d_1, and the curvature of the seed filling area is θ_4.

Diameter of the seed metering disc

The diameter of the seed metering disc is one of the key parameters of the seed metering device structure. It directly affects the installation positions of other components and the overall structural dimensions. During the seed filling process, the longer the holes on the seed metering disc remain in the seed filling area, the longer the seed filling time, which in turn increases the seed filling success rate and enhances the seed filling performance. The calculation formula for wheat seed filling time is as follows:

$$t_1 = \frac{30\theta_4}{\pi n_1} \quad \text{(Eq. 5)}$$

in which:

t_1- Seeding time, s ;

θ_4- Curvature of the filling area, rad;

n_1 - Rotational speed of the seeding disc, r/min.

From the calculation formula for seed filling time t_1, it can be concluded that the filling time is only related to the rotation speed of the seed metering disc and the curvature of the filling area. Increasing the diameter of the seed metering disc will increase the curvature of the filling area,

which leads to an increase in the number of holes that can be set on the seed metering disc. Based on design experience, the diameters of the seed metering discs used in traditional seed metering devices typically range from 140 to 260 mm (Chen *et al*., 2020). Considering that wheat seeds are small and have a regular shape, 1~2 rows of holes can be arranged on the seed metering disc. Therefore, the final diameter selected for the seed metering disc is 240 mm.

Hole shape on the seed metering disc

The distance from the edge of the seed metering disc to the center of the hole is generally 15~20 mm, and the distribution diameter of the holes is usually between 100~230 mm. Wheat seeds are small in size, so the position of the holes is set 15 mm from the edge of the seed metering disc at the outermost side of the hole diameter.

The shape of the holes on the seed metering disc has a significant impact on the negative pressure difference at both ends of the holes, directly influencing the quality of seed filling (Du and Liu, 2023). Fluent software was used to simulate and analyze different hole shapes, selecting the optimal shape based on the comparison of airflow velocities inside the holes (Wang *et al*., 2020). To ensure the validity of the comparison, only the shape was modified in the simulation model, while the hole depth and maximum diameter parameters were kept constant. The simulation parameters are as follows: the k-epsilon model was selected in the "Viscous" section, the inlet pressure at both ends of the hole was set to 0 kPa, the outlet pressure to -3 kPa, the fluid was set as air (incompressible), the viscosity was set to 1.7894×10^{-5} Pa·s, the specific heat capacity was 0.0242, and 300 iterations were calculated. The simulation results are shown in Figure 4.

From the analysis of the simulation results, it can be concluded that the maximum flow velocity at the outlet of the frustum-shaped hole and the cylindrical hole is almost identical. However, the gas flow velocity in the cylindrical hole remains uniform at around 70 m/s, while the airflow speed near the large circular end of the frustum-shaped hole decreases significantly, which negatively impacts the adsorption of wheat seeds. The "I"-shaped hole has the highest outlet flow velocity, but the airflow distribution inside the hole is highly irregular. Compared to the frustum-shaped hole, the gas flow speed at the edges of the "I"-shaped hole decreases more significantly, which is even less beneficial for seed adsorption. Additionally, the "I"-shaped hole is difficult to process in thinner seed metering discs. After comprehensive consideration, the cylindrical hole is selected as the optimal choice.

Hole diameter on the seed metering disc

The diameter of the holes on the seed metering disc is crucial for the negative pressure within the holes. When the negative pressure in the chamber is constant, if the hole diameter is too small, the negative pressure in the holes increases, enhancing the seed suction capability per

unit area. However, this reduces the suction area, which can cause large seeds to miss planting and small seeds to double plant. Conversely, if the hole diameter is too large, the negative pressure decreases, preventing seeds from being properly suctioned. Therefore, matching the hole diameter with the seed size is essential. The hole diameter is determined based on the seed size, using the empirical formula:

$$d_3 = (0.64 \sim 0.66)W \quad \text{(Eq. 6)}$$

where W is the average width of the wheat seed. From the previous section, the average width of Chuanmai 104 wheat seed is 3.58 mm. Using the formula, the hole diameter range is calculated to be 2.29 to 2.36 mm. Given the narrow range, 2.3 mm is chosen.

Hole depth design

The depth of the holes also corresponds to the thickness of the seed metering disc. To explore the effect of different hole depths on the suction capability for wheat seeds, Fluent software is used for simulation. The optimal hole depth is selected by comparing the airflow velocity inside the holes. For consistency, only the hole depth is modified in the simulation model, while the hole diameter and shape remain unchanged. The simulation parameters are as follows: inlet pressure is set to 0 kPa, outlet pressure to -2 kPa, the fluid is air (incompressible), viscosity is 1.7894×10^{-5}Pa·s, and specific heat capacity is 0.0242. The simulation results are shown in Figure 5, where it can be seen that different hole depths have almost no effect on the airflow velocity at the inlet, which remains between 56 and 58 m/s. Considering the overall structure of the seed metering device and the need for the seed metering disc to deform closer to the air groove edge under suction conditions, the hole depth and the thickness of the seed metering disc are selected as 1.5 mm.

Design of hole distribution and quantity

The number of holes on the seed metering disc is one of the most critical structural parameters. If the seeding speed and hole diameter are fixed, fewer holes require a higher rotation speed for the seed metering device, reducing seed filling time and potentially causing seeds to fall out due to collisions, leading to lower qualified seed filling rates. Conversely, more holes slow down the seed metering device's rotation, extending the seed filling process. However, too many holes increase the total cross-sectional area, raising the suction negative pressure, which can overburden the fan, sometimes preventing it from meeting the suction requirements (Liu *et al*., 2024). Therefore, a reasonable number of holes ensures good seeding performance. The calculation formula for the number of holes on the seed metering disc is as follows:

$$\begin{cases} M_z = \dfrac{1000^2 Q}{q} \\ S = \dfrac{100^2 D_d}{M_z B_c} \\ Z = \dfrac{\pi d_4 V_c (1+\zeta)}{V_1 S} \end{cases} \quad \text{(Eq. 7)}$$

Where:

Z - number of holes on the seed metering disc;

S - Wheat planting spacing , m;

M_z- seeds per hectare, seeds;

Q - seed rate per hectare, kg/hm^2;

q - thousand seed weight, g;

D_d - number of seed rows in the operating width;

B_c - operating width of the seeder, m;

d_4 - seed metering disc diameter, m;

V_c - seeder working speed, m/s;

ξ - seeder wheel slip ratio, 0.05~0.12;

V_1 - linear speed of the distribution circle of the holes on the seed metering disc, m/s.

According to the Agricultural Machinery Design Handbook (Chinese Academy of Agricultural Mechanization Sciences, 2007), the line speed of the seed hole distribution circle on the seed metering disc should generally not exceed 0.35 m/s, as exceeding this limit would significantly impair the seed metering performance. During precision wheat sowing, the seed sowing rate typically ranges from 105 to 135 kg/hm². The seeder's working width is selected as 1200 mm, with an operating speed of 3 km/h and 10 seed rows (Ali *et al*., 2010; Boström *et al*., 2012). Based on the aforementioned parameters, the calculated number of seed holes on the seed metering disc falls within the range of 33.51 to 46.55.

To further explore the structural parameters of air-suction precision wheat seeders and obtain the optimal parameter combination, factors such as air groove width, hole diameter, and number of holes are selected for experiments. Using the air velocity of the hole farthest from the negative pressure port in the seed filling area as the test indicator, an $L_9(3^4)$ orthogonal table is used for a three-factor, three-level orthogonal experiment in Fluent software (Yu, 2019). The factors and levels table are shown in Table 1.

A negative pressure airflow field model of the seed metering device is established. The air groove width is the width of a single airflow field after simplification, also the width of the negative pressure port. The model is saved in x_t. format and imported into Workbench. The simulation parameters are as follows: the k-epsilon model is selected in the "Viscous" section,

the holes are set as the inlet with 0 kPa pressure, the negative pressure port as the outlet with -2 kPa pressure, other surfaces as walls, the fluid is air (incompressible), viscosity is 1.7894×10^{-5} Pa·s, and specific heat capacity is 0.0242. After 300 iterations, the simulation results are shown in Figure 6, and the experiment scheme and results are in Table 2.From the range analysis, it can be seen that the sequence of factors affecting airflow velocity is as follows: air groove width > hole diameter on the seed metering disc > number of holes on the seed metering disc. The factor-criterion diagram for the results of this experiment is shown in Figure 7.

To improve the index levels, the optimal combination of parameters should be selected. According to the Index-factor diagram, the optimal parameter combination obtained is $A_2B_2C_2$, meaning the air groove width is 15 mm, the hole diameter on the seed metering disc is 2.3 mm, and the number of holes is 36.

Force analysis in the seed filling area

For wheat seeds in the seed filling area of the seed metering device, a sufficient pressure difference is required to generate an adhesion force strong enough to allow the seed metering disc to exert sufficient friction to counteract other forces. The state of adhesion means that the wheat seeds are in force equilibrium. When the seeds are being filled, the force analysis diagram for a single wheat seed when adhered to the hole on the seed metering disc is shown in FIG 8. For the seed filling stage, the adhesion force required to hold a single wheat seed in the hole must satisfy the following:

$$H_x = \frac{N}{S_x}(1) \quad \text{(Eq. 8)}$$

In the formula:

$$\begin{cases} \dfrac{Nd_3}{2} = Vc \\ S_x = \dfrac{\pi {d_3}^2}{4} \\ V = \sqrt{U^2 + {G_m}^2 + 2\cos\theta_1 U G_m} \\ U = \sqrt{{F_c}^2 + {F_f}^2} \\ F_c = \dfrac{G_m V_1^2}{Gd_2} \end{cases} \quad \text{(Eq. 9)}$$

in which:

H_x - negative pressure in the hole, Pa;

S_x - area of the hole, m^2;

N - adhesive force exerted by the seeding disc holes on the wheat seed, N;

d_3 - diameter of the hole, m;

V - combined force of friction force Ff, centrifugal force Fc and gravity Gm acting on the wheat seed, N;

c - distance from the wheat seed's center of mass to the plane of the seeding disc, m;

θ_1 - angle between U and Gm,°;

V_l - linear velocity of the hole distribution circle, m/s;

G - acceleration due to gravity, assumed as 9.8 m/s^2;

G_m - gravity acting on the wheat seed, N;

F_f - frictional force exerted by the seeding disc on the wheat seed, N;

F_c - centrifugal force experienced by the wheat seed when the seeding disc rotates, N;

U - combined force of friction force Ff and centrifugal force Fc, N;

The negative pressure in the hole is:

$$H_x = \frac{8cK_1K_2}{\pi d_3^{\,3}}\sqrt{F_f^{\,2} + G_m^{\,2} + \frac{G_m^{\,2}V_l^4}{g^2 d_2^{\,2}} + 2\cos\theta_1 G_m\sqrt{\frac{G_m^{\,2}V_l^4}{gd_2^{\,2}} + F_f^{\,2}}} \quad \text{(Eq. 10)}$$

Where:

K1 - Seeder working reliability coefficient, ranging from 1.6 to 2.0;

K2 – The Reliability coefficient of seed suction,r anging from 1.8 to 2.0.

Based on the analysis, the maximum value of H_x can be achieved when K1, K2, and cosθ1 are maximized. The maximum value of the negative pressure in the hole is:

$$H_{x\max} = \frac{8G_mK_1K_2}{\pi d_3^{\,3}}\sqrt{1+\tau+\frac{V_l 2}{gd_2}} \quad \text{(Eq. 11)}$$

In the formula:

$$\tau = (6 \sim 10)\,tan\,\psi \quad \text{(Eq. 12)}$$

in which:

H_{xmax} – maximum negative pressure in the hole, Pa;

τ – wheat comprehensive friction coefficient;

ψ - natural repose angle of wheat, °.

From Eq. 11 it can be concluded that the negative pressure in the hole is only related to the hole diameter, seed metering disc rotational speed, and the material properties of the wheat seed.

Optimization of seeder work parameters

Test equipment and preparation

The experiments use *Chuanmai* 104 wheat seeds, with seed spacing between 0.16 to 0.27 m. The tests are conducted on an air-suction precision wheat seed metering device. The air pressure at the holes is monitored and measured using a wind speed, pressure, and airflow testing device. The seed metering disc rotation speed is controlled by a motor-driven chain sprocket, and the tilt angle of the seed metering device is adjusted by altering the fixture position. The seed metering test rig is shown in Figure 9.

Test factors and indicators

During the operation of the air-suction precision wheat seed metering device, different operating parameters will result in varying work quality. To further explore the seed metering quality of the air-suction precision wheat seed metering device, a study was conducted on the impact of different working parameters on the seeding results. The test factors include hole negative pressure, seed metering disc rotational speed, and tilt angle of the seed metering device, with the test indicators being the qualified rate index, multiple index, and missed index. A quadratic regression rotating orthogonal test was conducted, and the experimental data was subjected to regression analysis to establish regression equations. Response surface analysis was performed to optimize the test data and determine the optimal combination of operating parameters for the seed metering device.

Hole negative pressure: when the hole negative pressure is low, the adhesion force generated at the holes is weak, causing wheat seeds to either fail to adhere to the seed metering disc or fall off with slight vibrations, leading to a high missed index. As the negative pressure increases, the wheat seeds gradually adhere to the seed metering disc, resulting in an increase in the qualified index and a decrease in the missed and multiple indices. However, when the negative pressure further increases, the adhesion force becomes strong enough to hold multiple wheat seeds, causing a more significant rise in the multiple index beyond 1150 Pa. The overall optimal effect is observed within the 850~1150 Pa range.

Seed metering disc rotational speed: Preliminary experiments found that when the seed metering disc speed is low, the time the holes spend in the filling area increases, causing multiple wheat seeds to adhere to the holes, resulting in a high multiple index. As the speed increases, the situation improves, but if the speed becomes too high, the time spent in the filling area becomes too short, leading to the wheat seeds not having enough time to be suctioned before the holes move to the carrying area, significantly increasing the missed index. The qualified index and multiple index decrease as a result. When the seed metering disc speed is between 40 and 50 r/min, the qualified index of the air-suction precision wheat seed metering device exceeds 80%, indicating good seeding performance.

Tilt angle of the seed metering device: It was observed that when the tilt angle is negative, some wheat seeds, due to gravity, flow toward the holes, causing multiple seeds to adhere to the holes, resulting in a higher multiple index. As the tilt angle increases from zero, the number of seeds at the holes decreases, and the missed index rises. When the tilt angle is 0° (i.e., the seed delivery pipe is vertical), the qualified index of the air-suction precision wheat seed metering device exceeds 80%, demonstrating good seeding performance.

The seeding quality indicators are processed according to the national standard of the People's Republic of China, Norm GB/T 6973-2005 (General Administration of Quality Supervision, 2005).

Orthogonal experiment

Orthogonal experiment design

The experimental factors include hole vacuum pressure, seed metering disc rotation speed, and inclination angle, while the experimental indicators are qualified index (X), missed seeding index (Y), and multiple seeding index (Z). A three-factor quadratic regression rotational orthogonal experiment was conducted, and the factor levels and coding are shown in Table 3.

Experimental results and analysis

The orthogonal experiment plan and results are shown in Table 4 (A, B, and C represent the factor level values, while X, Y, and Z represent the missed seeding rate, multiple seeding rate, and qualified rate, respectively). The data from Table 4 were fitted with multiple regression analysis using Design-Expert software, and the regression analysis of variance is shown in Table 5.

The regression equations for the qualified index X, missed sowing index Y, and re-sowing index Z are as follows:

$$\begin{cases} X = 90.13 + 2.01B - 3.1A^2 - 3.56B^2 - 2.34C^2 \\ Y = 4.44 + 4.58A + 2.23B - 1.55C - 1.83AB \\ \quad +2.31A^2 + 4.84B^2 + C^2 + 1.17ABC - 8.25A^2B - 2.73AB^2 \\ Z = 5.28 - 3.45A - 2.35B + 2.71C + 1.28A^2 2.22B^2 + 1.83C^2 \\ \quad -1.55ABC + 5.02A^2B + 2.02AB^2 - 2.2A^2B^2 \end{cases} \quad \text{(Eq. 13)}$$

The order of factors affecting the qualified index is: seed metering disc rotation speed, inclination angle, and hole vacuum pressure. The order of factors affecting the missed seeding index is: seed metering disc rotation speed, hole vacuum pressure, and inclination angle. The order of factors affecting the multiple index is: hole vacuum pressure, inclination angle, and seed metering disc rotation speed.

Using Design-Expert software, response surface analysis of the experimental data was

conducted, showing the effects of the interactions between hole vacuum pressure, seed metering disc rotation speed, and inclination angle on the qualified index, missed seeding index, and multiple seeding index, as shown in Figure 10. The average qualified index obtained from the experiment was 78.38%, the average missed seeding index was 12.41%, and the average multiple index was 9.21%.

Parameter optimization

By optimizing the data through software, the optimization plan set the qualified index to be greater than 89%, and the missed seeding index and multiple seeding index to be less than 5.5%. The software calculated the optimal parameter range, as shown in Figure 11. When the inclination angle is 0°, the yellow region represents the best parameter zone, with a seed metering disc rotation speed of 43.8~47 r/min and a hole vacuum pressure of 960-1040 Pa, which satisfies the optimized conditions for the qualified index, missed seeding index, and multiple seeding index.

Validation experiment

The optimized parameters were verified through a test stand experiment, where the seed metering disc rotation speed was set to 45 r/min, hole vacuum pressure to 1000 Pa, and inclination angle to 0°. Five repeated tests were conducted to validate the optimization results. The results showed that the average qualified index of the air-suction wheat precision seed metering device was 90.7%, the average missed seeding index was 4.8%, and the average multiple seeding index was 4.5%. Compared to the pre-optimization results, the average qualified index increased by 15.7%, the missed seeding index decreased by 61.3%, and the multiple seeding index decreased by 51.1%, which largely met the optimization expectations.

Conclusions

This study designs an air-suction wheat precision seed metering device. The diameter of the seed metering disc, hole position, number of holes, and hole diameter are determined through theoretical calculations and empirical formulas.

Based on Fluent software, the internal gas flow field of the air-suction wheat precision seed metering device was simulated and tested. The optimal dimensional parameter combination for the seed metering disc was determined: cylindrical holes with a depth of 1.5 mm, a diameter of 2.3 mm, 36 holes, and a gas flow slot width of 15 mm. The influence sequence of the gas flow slot width, hole diameter, and number of holes on the airflow velocity through the holes was also determined.

A second-order regression rotational orthogonal experiment was conducted for three factors:

hole negative pressure, seed metering disc speed, and inclination angle. The impact order of these factors on the qualification rate, missed seed rate, and multiple seed rate was obtained. Corresponding regression equations were calculated and analyzed. The data were optimized using software, with the conditions that the qualification index be greater than 89% and both the missed seed rate and multiple seed rate be less than 5.5%. The optimal operational parameters were found to be: inclination angle of 0°, seed metering disc speed of 43.8-47 r/min, and hole negative pressure of 960-1040 Pa.

A bench test was conducted with the optimized parameters: inclination angle of 0°, seed metering disc speed of 45 r/min, and hole negative pressure of 1000 Pa. The results showed that, compared to the pre-optimization parameters, the average qualification index increased by 15.7%, the average missed seed rate decreased by 61.3%, and the average multiple seed rate decreased by 51.1%, demonstrating the ideal outcome of the optimization.

References

Ali, M., Ali, L., Sattar, M., Ali, M.A. 2010. Improvement in wheat (Triticum aestivum L.) Yield by manipulating seed rate and row spacing in Vehari zone. J. Anim. Plant Sci. 20:225-230.

Boström, U., Anderson, L.E., Wallenhammar, A.C. 2012. Seed distance in relation to row distance: Effect on grain yield and weed biomass in organically grown winter wheat, spring wheat and spring oats. Field Crop. Res. 134:144-152.

Chen, H., Wang, H., Wang, Y., Shi, N., Wei, Z., Dou, Y. 2020. Design and experiment of axial air-suction drum seed-metering device. Trans. Chin. Soci. for Agr. Machin. 51:75-85.

Chen, S., Liu, Y., Song, Z., Xie, F., Sun, Q. 2019. Finite element analysis of the flow field in the air chamber and the orifice of the air suction metering device. J. Agr. Mechan. Res. 41:64-68.

Chinese Academy of Agricultural Mechanization Sciences, 2007. Handbook of Agricultural Machinery Design. China Agricultural Science and Technology Press. Beijing, China.

Du, X., Liu, C. 2023. Design and testing of the filling-plate of inner-filling positive pressure high-speed seed-metering device for maize. Biosyst. Eng. 228:1-17.

General Administration of Quality Supervision, 2005. Testing methods of single seed drills (precision drills). Norm GB/T 6973-2005. Standards Press of China, Beijing, China.

Guarella, P., Pellerano, A., Pascuzzi, S. 1996. Experimental and theoretical performance of a vacuum seeder nozzle for vegetable seeds. J. Agr. Eng. Res. 64:29-36.

Jadhav, M., Din, M., Nandede, B., Kumar, M. 2020. Engineering properties of paddy and wheat seeds in context to design of pneumatic metering devices. J. Inst. Engin. (India) Series A. 101:281-292.

Leng, J., Liu, F., Zhang, T., Jia, Y. 2023. Experimental study on seed discharging performance of air suction precision metering device for sorghum. J. Hebei Agri. Univ. 46:109-114.

Li, D., Jin, H., Lei, D., Ren, S. 2023. Research progress on pneumatic corn precision seed-metering device in China. Modern Agr. Sci. Technol. 136-138.

Li, Z., Lei, X., Cao, X., Liao, Y., Liao, Q., Li, S. 2015. Design and experiment of pneumatic-typed precision centralized metering device for rapeseed. Trans. Chin. Soc. Agr. Eng. 31:9-17.

Li, Z., Zhang, H., Huang, J., Lou, C., Chen, Y., Liu, L., Zhang, T., Chen, L. 2025. Design and parameter optimization of air-delivery auxiliary seed guide for pneumatic plate precision rapeseed metering device. Comput. Electron. Agric. 230:109840.

Liu, X., Su, C., Li, Z., Wang, K., Xie, F., Tian, Y., Qi, J. 2024. Analysis and evaluation of seed-filling performance of a pneumatic interference precision seeder for small cabbages. Appl. Sci. 14:2825.

Shi, B., Cheng, D., Kang, Z. 2020. Design of automatic replanting device for leaky seeding of precision planter. J. Agr. Mechan. Res. 42:137-140.

Singh, R.C., Singh, G., Saraswat, D.C. 2005. Optimisation of design and operational parameters of a pneumatic seed metering device for planting cottonseeds. Biosyst. Eng. 92:429-438.

Tang, H., Xu, F., Guan, T., Xu, C., Wang, J. 2023. Design and test of a pneumatic type of high-speed maize precision seed metering device. Comput. Electron. Agric. 211:107997.

Wang, C., Ma, X., Jia, R. 2009. Effects of working parameters on seed suction performance of seeder device for super hybrid rice seeds. Trans. Chin. Soc. Agr. Eng. 25:88-92.

Wang, F., Sun, K., Lai, Q., Dong, J., Su, W., Yu, Q. 2020. Design and experiment of minituber precision single-row air-suction planter. Trans. Chin. Soc. Agr. Machin. 51:66-76.

Xing, H., Zang, Y., Cao, X., Wan,g Z., Luo, X., Zeng, S., Huang, M. 2015. Experiment and analysis of dropping trajectory on rice pneumatic metering device. Trans. Chin. Soc. Agr. Eng. 31:23-30.

Yasir, S.H., Liao, Q., Yu, J., He, D. 2012. Design and test of a pneumatic precision metering device for wheat. CIGR J. 14:16-25.

Yu, G. 2009. Chinese Academy of Agricultural Sciences Dissertation. New West. 31-33.

Yu, Q. 2019. Design and experiment of precisionair-suction cell-wheel seed metering device for Panax notoginseng. Degree Diss. Kunming University of Science and Technology,

Zhang, M., Ma, Q., Ding, J., Li, C., Zhu, X., Feng, C., Guo, W. 2018. Characteristic of late sowing high-yielding wheat population in rice-wheat rotation. J. Triticeae Crops 38:445-454.

Zhu, J., Liu, J., Fu, Y., Xi, Y. 2023. Design and experiment of a suction type millet precision seed meter. J. Hebei Agr. Univ. 46:111-117.

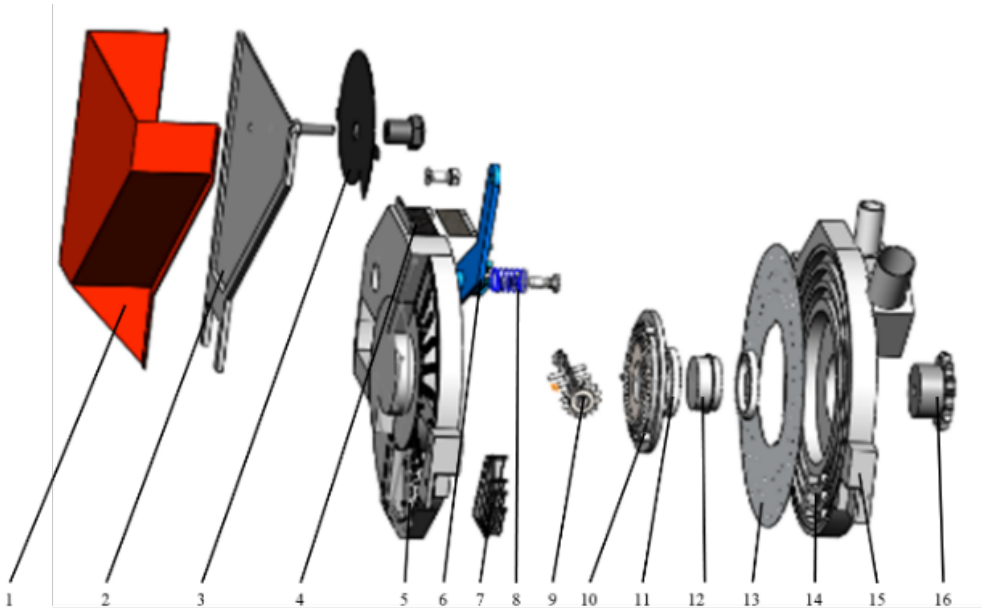

Figure 1. Schematic diagram of the seed metering device structure. 1. Seed box; 2. seed box connecting plate; 3. adjustment scale plate; 4. sealing brush; 5. seed box end housing; 6. brushing plate; 7. seeding support pipe; 8. adjustment spring; 9. stirring shaft; 10. conical gear plate; 11. seeding shaft bearing, 12. seeding shaft; 13. seeding disc; 14. negative pressure air groove; 15. negative pressure end housing; 16. seeding shaft sprocket.

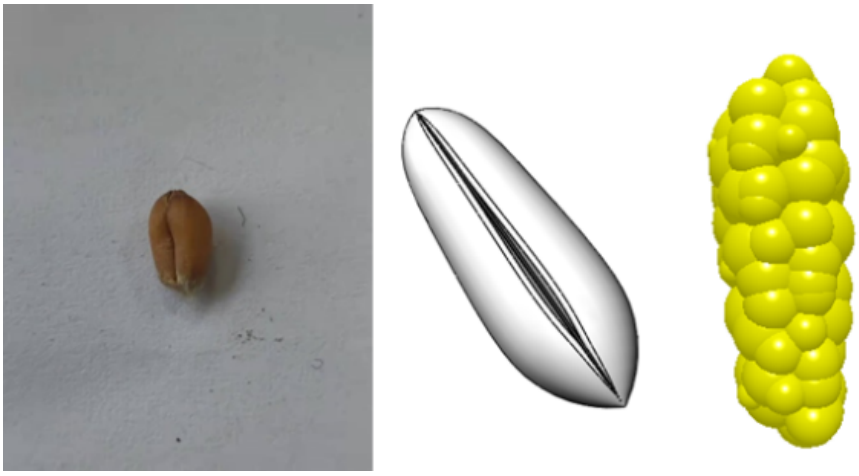

Figure 2. Wheat seed, 3D model, and particle model.

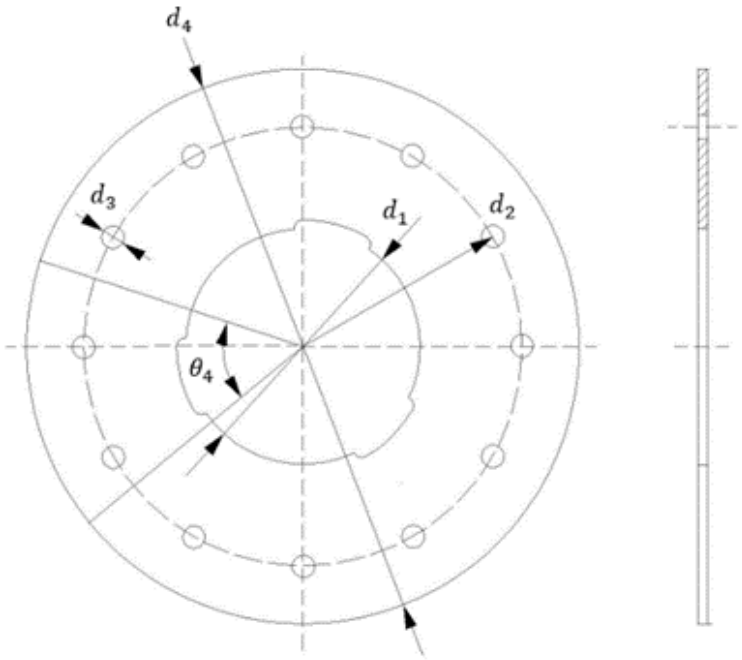

Figure 3. Structure diagram of seed plate.

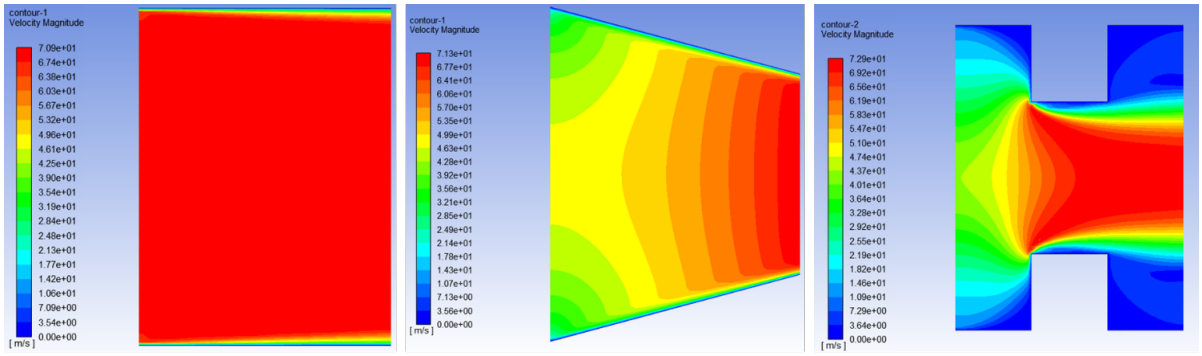

a. Cylindrical hole b. Frustum-shaped hole c. I-shaped hole

Figure 4. Airflow velocity cloud diagram of the hole on the seed metering disc.

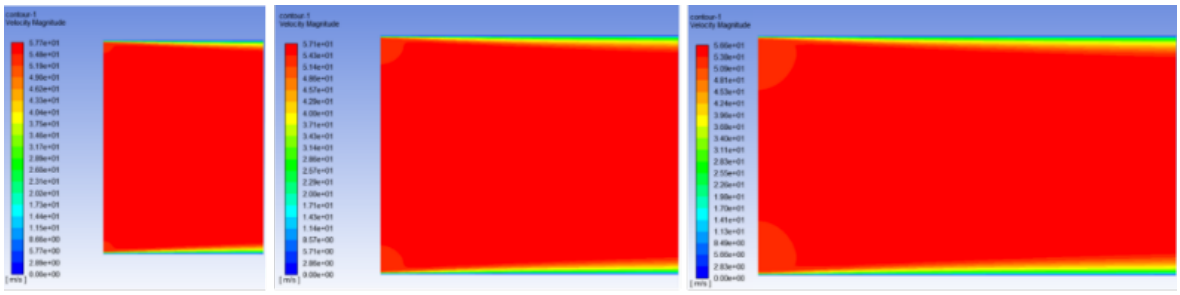

Figure 5. Airflow velocity cloud diagram for different hole depths.

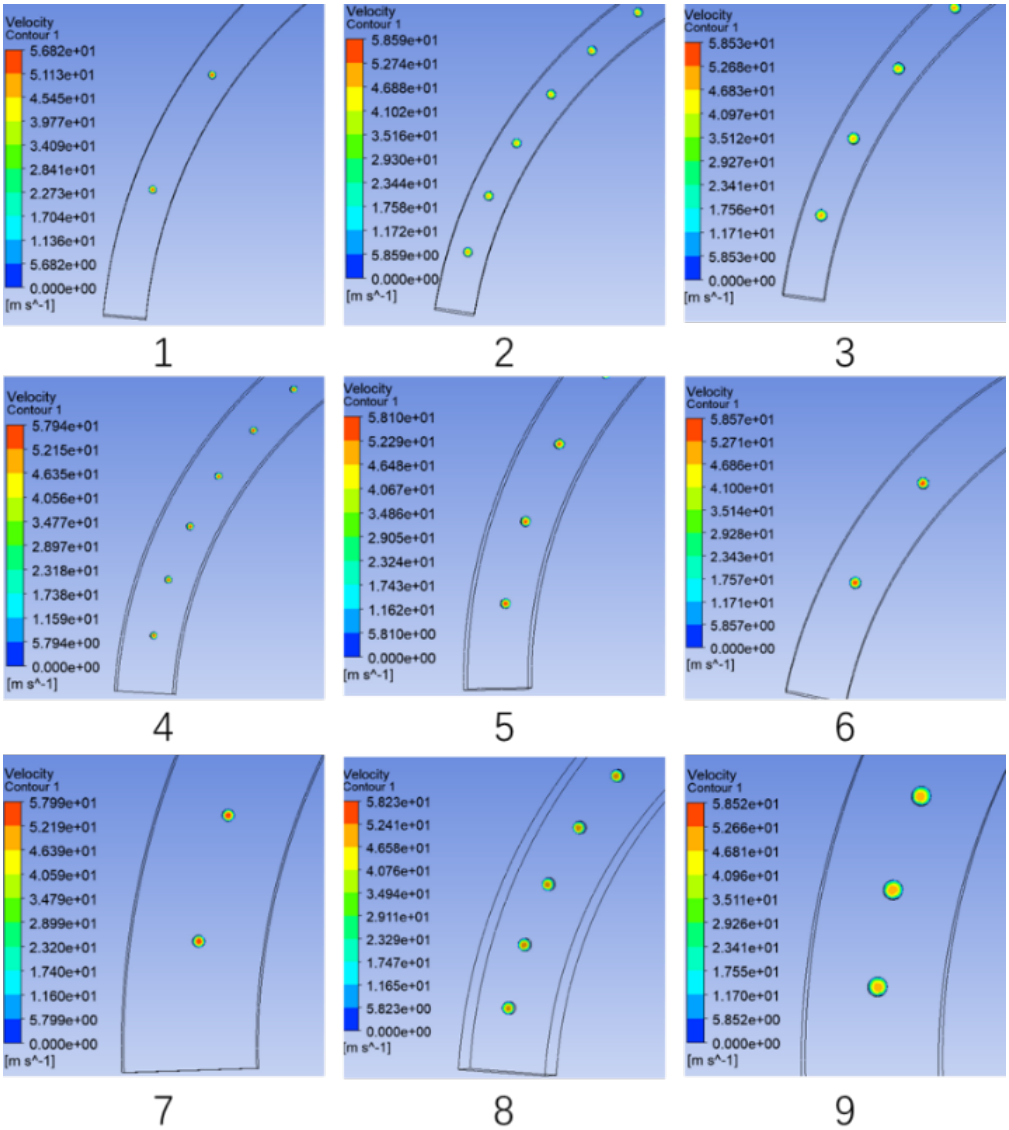

Figure 6. Airflow velocity cloud diagram of the hole on the seed metering disc.

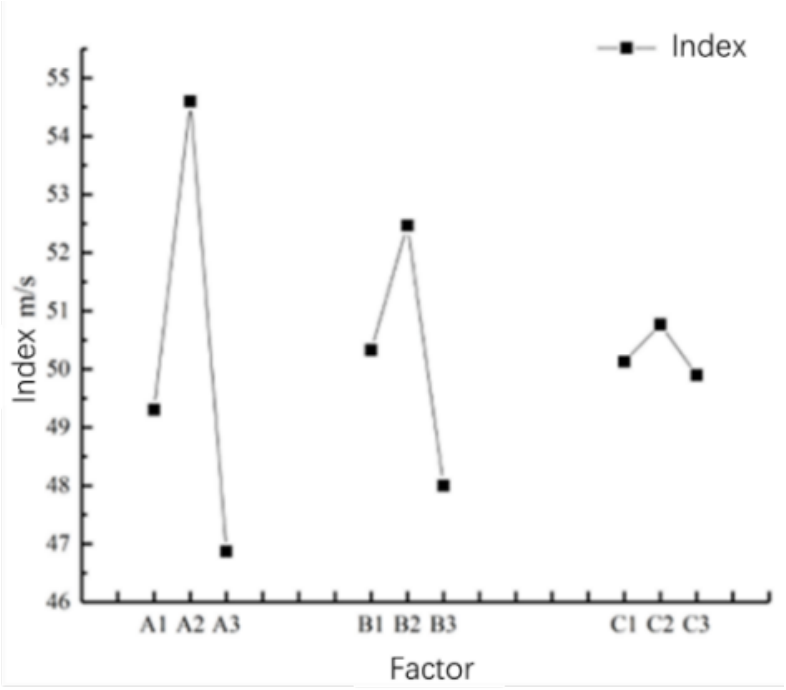

Figure 7. Index-factor diagram.

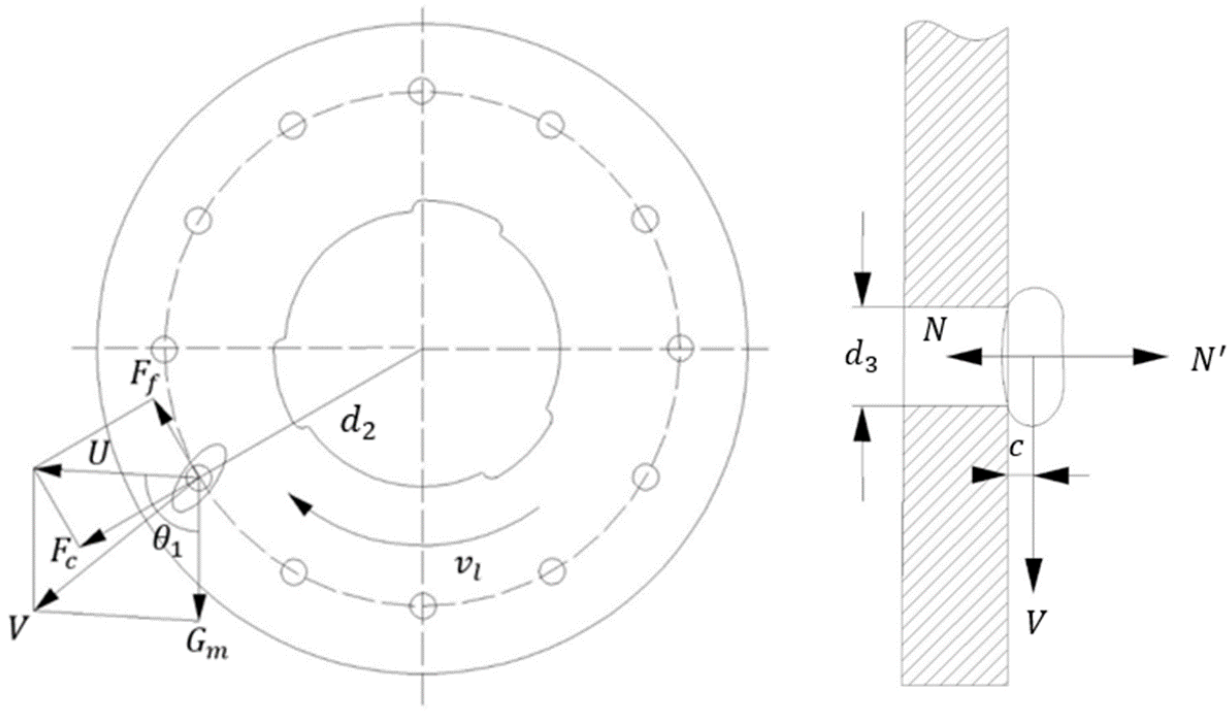

Figure 4. Schematic diagram of the force analysis on the seed.

Figure 5. Test bench for the air-suction precision wheat seed metering device. 1. Wind turbine control system; 2. pneumatic wheat precision seeder; 3. seeder performance testing stand; 4. wind speed and airflow meter.

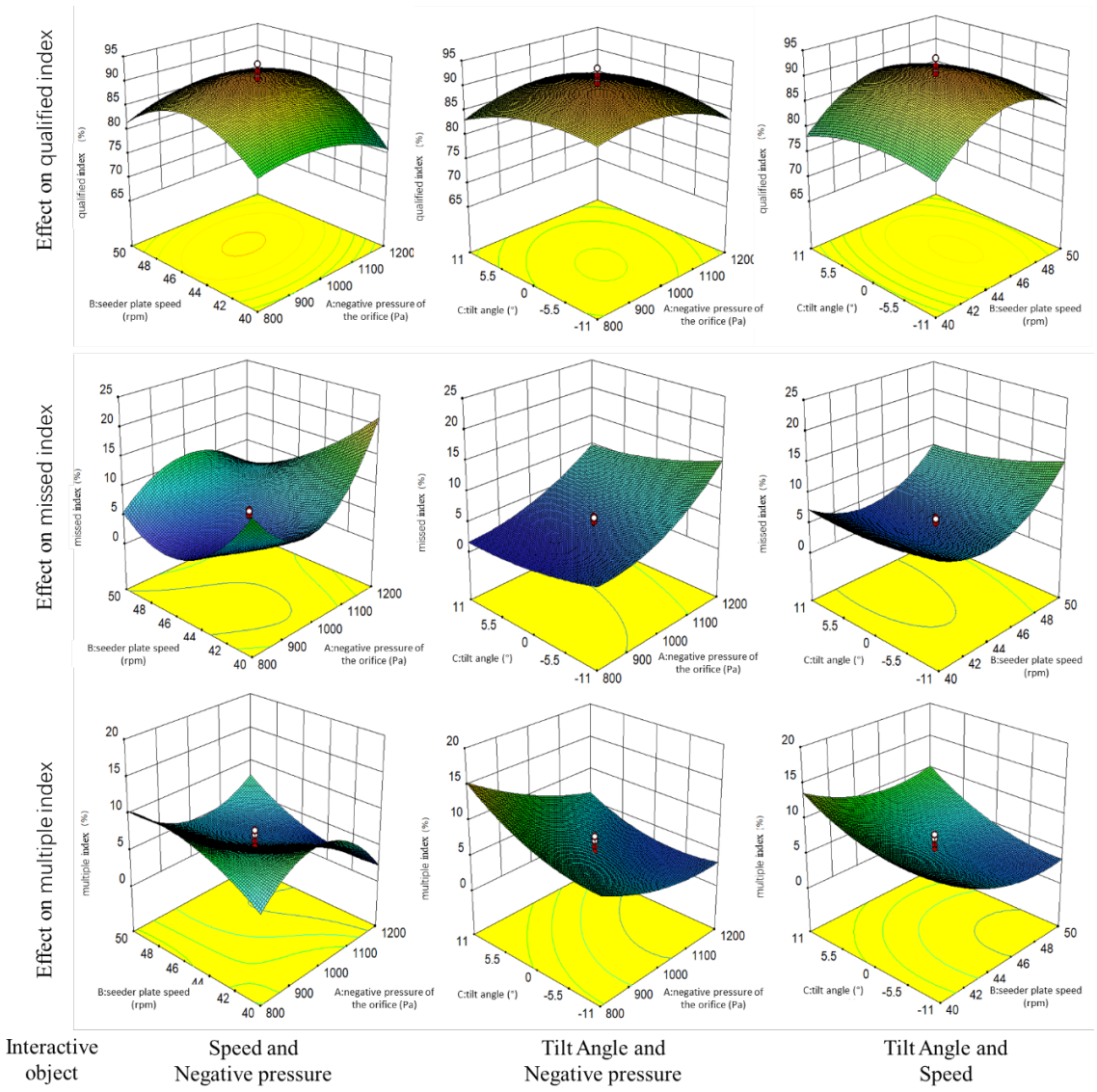

Figure 6. Response surface.

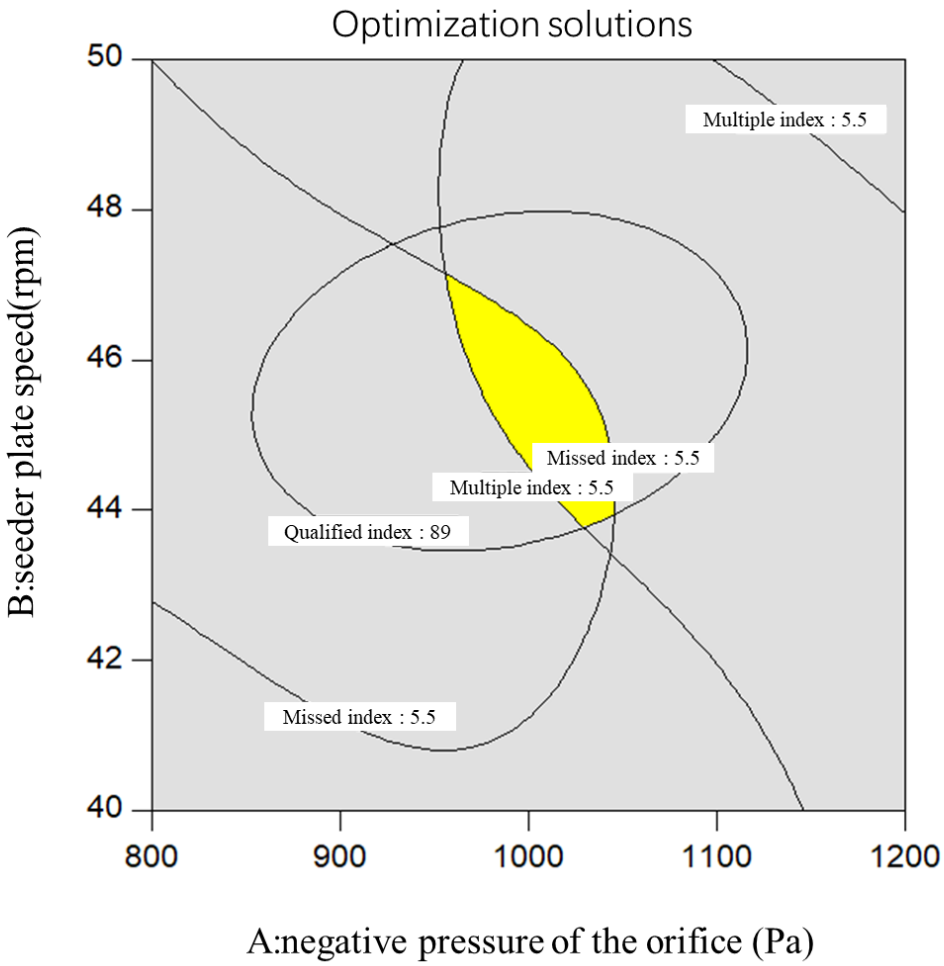

Figure 7. Parameter optimisation analysis.

Table 1. Levels and factors of the simulation experiment.

	Width of the airflow groove A/(mm)	Diameter of the hole B/(mm)	Number of holes C/(unit)
1	10	1.8	24
2	15	2.3	36
3	20	2.8	48

Table 2. Simulation experiment plan and results.

Test number	Factor			Airflow velocity in the hole y(m/s)
	A	B	C	
1	1	1	1	51.6
2	1	2	2	49.1
3	1	3	3	47.3
4	2	1	2	57.9
5	2	2	3	54.5
6	2	3	1	51.4
7	3	1	3	47.9
8	3	2	1	47.4
9	3	3	2	45.3
y K1	148	157.4	150.4	
y K2	163.8	151	152.3	
y K3	140.6	144	149.7	
y R	7.733333	4.466667	0.866667	

Table 3. Test factors and levels.

Level	Factor		
	Negative pressure of the hole A (Pa)	Rotation speed of the seed tray B（r/min）	Tilt Angle C（°）
-1.682	664	36.6	-18.5
-1	800	40	-11
0	1000	45	0
1	1200	50	11
1.682	1336	53.4	18.5

Table 4. Test result.

Number	Factor			X(%)	Y(%)	Z(%)	Number	Factor			X(%)	Y(%)	Z(%)
	A	B	C					A	B	C			
1	-1	-1	-1	79.8	14.2	6							
2	1	-1	-1	73.4	24.8	1.8	13	0	0	-1.682	83.8	10.3	5.9
3	-1	1	-1	83.6	9.8	6.6	14	0	0	1.682	79.9	5.1	15
4	1	1	-1	82.4	8.4	9.2	15	0	0	0	87.8	5.3	6.9
5	-1	-1	1	76.3	15.1	8.6	16	0	0	0	91.6	2.4	6
6	1	-1	1	74.3	19.2	6.5	17	0	0	0	86.8	5.7	7.5
7	-1	1	1	79.2	2.7	18.1	18	0	0	0	90.1	4.6	5.3
8	1	1	1	85.4	4.2	10.4	19	0	0	0	90.7	5.1	4.2
9	-1.682	0	0	81.6	3.7	14.7	20	0	0	0	90.5	4.7	4.8
10	1.682	0	0	77.8	19.1	3.1	21	0	0	0	92.1	4.1	3.8
11	0	-1.682	0	69.7	14.8	15.5	22	0	0	0	88.6	5.5	4.9
12	0	1.682	0	70.1	22.3	7.6	23	0	0	0	93.5	2.4	4.1

Table 5. Analysis of variance of regression equation.

Test index	Source of variance	Sum of squares	Degree of freedom	F	P
Qualified rate	A	7.02	1	0.88	0.3641
	B	55.27	1	6.97	0.0204*
	C	8.16	1	1.03	0.3289
	AB	22.44	1	2.83	0.1164
	AC	17.4	1	2.19	0.1624
	BC	0.18	1	0.023	0.8826
	A^2	152.56	1	19.23	0.0007**
	B^2	684.48	1	86.28	<0.0001**
	C^2	86.89	1	10.95	0.0056**
	Residual error	103.14	13		
	Lack of fit	66.45	5	2.9	0.0877
	error	36.69	8		
	Sum total	1128.26	22		
Missed rate	A	118.58	1	75.26	<0.0001**
	B	28.12	1	17.85	0.0022**
	C	13.52	1	8.58	0.0168*
	AB	26.64	1	16.91	0.0026**
	AC	1.62	1	1.03	0.3371
	BC	5.45	1	3.46	0.096
	A^2	85	1	53.95	<0.0001**
	B^2	372.35	1	236.33	<0.0001**
	C^2	16.04	1	10.18	0.0110*
	ABC	11.05	1	7.01	0.0266*
	A^2B	225.8	1	143.31	<0.0001**
	A^2C	0.68	1	0.43	0.5267
	AB^2	24.67	1	15.66	0.0033**
	Residual error	14.18	9		
	Lack of fit	1.76	1	1.14	0.3174
	error	12.42	8		
	Sum total	1038.37	22		
Multiple rate	A	67.28	1	40.79	0.0002**
	B	31.21	1	18.92	0.0024**
	C	41.41	1	25.1	0.0010**
	AB	0.18	1	0.11	0.7496
	AC	8.41	1	5.1	0.0539
	BC	3.65	1	2.21	0.1754
	A^2	21.47	1	13.02	0.0069**

B^2	64.38	1	39.03	0.0002**
C^2	43.78	1	26.54	0.0009**
ABC	19.22	1	11.65	0.0092**
A^2B	83.63	1	50.7	<0.0001**
A^2C	0.14	1	0.085	0.7783
AB^2	13.57	1	8.23	0.0209*
A^2B^2	15.53	1	9.42	0.0154*
Residual error				
Lack of fit error	13.2	8		
Sum total	412.38	22		

*p<0.05,**p<0.01.